Phys. Status Solidi A **210**, No. 3, 455–458 (2013) / **DOI** 10.1002/pssa.201200476

physica status solidi a
www.pss-a.com
applications and materials science

Cubic III-nitride coupled quantum wells towards unipolar optically pumped lasers

C. Mietze*[,1], M. Bürger[1], S. Sakr[2], M. Tchernycheva[2], F. H. Julien[2], and D. J. As[,1]**

[1] Department of Physics, University of Paderborn, Warburger Str. 100, 33095 Paderborn, Germany
[2] Institut d'Electronique Fondamentale, UMR 8622 CNRS, University Paris-Sud 11, 91405 Orsay, France

Received 13 July 2012, revised 20 December 2012, accepted 10 January 2013
Published online 30 January 2013

Keywords cubic III-nitrides, intersubband transitions, molecular beam epitaxy, superlattices

* Corresponding author: e-mail cmietze@mail.upb.de, Phone: +49 5251 605828, Fax: +49 5251 605843
** e-mail d.as@uni-paderborn.de, Phone: +49 5251 605838, Fax: +49 5251 605843

Optical and structural properties of asymmetric coupled cubic-GaN/-AlN quantum wells (QW) are studied. The samples are grown by molecular beam epitaxy on a 50 nm c-GaN buffer on 3C-SiC substrate. The active region contains 100 periods of a 2.3 nm AlN barrier, a 1.9–2.1 nm silicon doped GaN QW and a 1.0–1.2 nm undoped GaN QW coupled by a 0.9–1.1 nm AlN tunnelling barrier. Phase purity and partial relaxation of the superlattice is observed in reciprocal space maps measured by high resolution X-ray diffraction. Optical properties of coupled QWs are investigated using cathodoluminescence spectroscopy. A clear shift in the emission energy associated with the thickness of the QWs can be observed. Furthermore clear TM-polarized infrared absorption in the 0.55–0.87 eV range is observed at room temperature using Fourier transform infrared spectroscopy. The asymmetric shape of the infrared absorptions reveals the existence of a three level system in the QWs and is explained by contributions of the e1–e3 and e2–e3 intersubband transitions. Measured transition energies are compared to model calculations using a Schrödinger–Poisson solver based on an effective mass model (nextnano^3).

© 2013 WILEY-VCH Verlag GmbH & Co. KGaA, Weinheim

1 Introduction Today III-nitrides are the material of choice for manifold device applications like light emitting diodes, laser diodes or field-effect transistors. Due to the large conduction band discontinuity between AlN and GaN, novel nitride-devices based on intersubband transitions (ISBT), like quantum well (QW) infrared photo detectors [1], quantum cascade lasers (QCLs) [2] or optically pumped quantum fountain lasers (QFLs) [3] operating at telecommunication wavelengths are proposed. Presently the research on ISB devices is mainly focused on wurtzite nitrides. Coupling between GaN/AlN wurtzite QWs has been reported [4]. Due to the hexagonal symmetry strong intrinsic piezoelectric and pyroelectric fields are present in nitride heterostructures. These built-in fields reduce the transition probability in QWs and are therefore undesirable in optical devices. In multi-quantum-wells (MQW) or superlattices (SL) these internal fields introduce a strong band bending complicating the design and limit the tunability of ISBT energies. Hence the growth of non-polar and semi-polar nitrides has found increasing interest in the last years to avoid these strong internal fields. However, the electrical, optical and structural properties show strong lateral anisotropy since the polarization field is now in the plane of growth. An alternative way to fabricate group III-nitrides without spontaneous polarization fields is the growth of meta-stable non-polar cubic group III-nitrides [5–7]. During the last years, a lot of preliminary work towards unipolar optoelectronic devices like QCL or optically pumped lasers based on cubic nitrides has been carried out. The large band-offset between c-GaN and c-AlN has been determined [8]. Intersubband absorption in the near-infrared to terahertz spectral range was measured [9, 10] and resonant tunnelling through c-AlN double barriers was shown [11, 12]. These achievements form a solid base for development of future optically pumped lasers based on cubic group III-nitrides.

2 Principle of an optically pumped laser In an optically pumped laser like a QFL selective optical excitation is used to promote electrons from the ground state to an excited state of the active QWs [3]. The operation of an optically pumped laser relies on the radiative transition of electrons between bound states of asymmetric coupled quantum wells (ACQW). The calculated conduction band profile of an appropriate ACQW system of cubic III-nitrides is shown in Fig. 1. Population of the ground state e1 can be

© 2013 WILEY-VCH Verlag GmbH & Co. KGaA, Weinheim

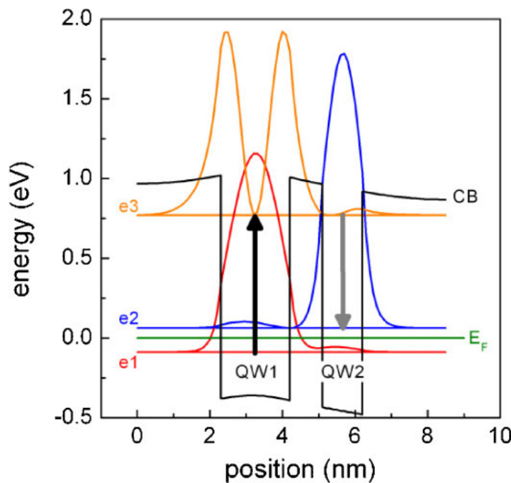

Figure 1 (online colour at: www.pss-a.com) Calculated conduction band edge for one ACQW period of sample A (black line) and quantized states including squared wave functions.

achieved by Si-doping. The optical pumping takes place from state e1 to the second excited state e3 while emission occurs from e3 to the second excited state e2 (transitions indicated by arrows in Fig. 1). To achieve population inversion between e3 and e2 the lifetime of electrons in state e2 has to be shorter than the scattering time between e3 and e2 [13]. Fast depopulation of e2 state can be achieved by resonant phonon scattering if the e1–e2 energy separation is adjusted to be of the order of the LO phonon energy (92 meV in c-GaN [14]). In the following, we will present first experimental results on the growth and characterization of cubic III-nitride ACQW showing the promise of III-nitrides for future optically pumped laser devices.

3 Experimental

3.1 Sample description Four samples were fabricated in a Riber32 plasma assisted molecular beam epitaxy machine. We use a 10 μm thick 3C-SiC substrate grown on 500 μm Si. Details on the growth can be found in Ref. [15]. The samples consist of a 50 nm c-GaN buffer grown on 3C-SiC. The active region is formed by a 2.3 nm c-AlN barrier, a silicon doped c-GaN QW with a thickness varied from 1.9 to 2.1 nm and a 1.0–1.2 nm undoped c-GaN QW coupled by a 0.9–1.1 nm c-AlN barrier. Structural properties of the samples are summarized in Table 1.

Table 1 List of samples with thicknesses of the single layers.

sample	GaN QW1 (nm)	GaN QW2 (nm)	AlN tunnelling barrier (nm)
A	1.9	1.1	0.9
B	1.9	1.0	1.1
C	2.0	1.2	0.9
D	2.1	1.1	1.1

3.2 Model calculations For a more detailed understanding and modelling of future devices it is essential to perform band structure calculations. The calculations shown in this work are performed using nextnano[3] [16]. Band structures and localized states are calculated using an effective mass model. Figure 1 shows the calculated conduction band edge of sample A in combination with the squared wave functions of electrons of three localized states e1, e2 and e3. The Fermi level (E_F) is slightly above the e1 state but still below the e2, in order to provide strong e1–e3 pump absorption while avoiding e2–e3 emission reabsorption. From the squared wave functions one can clearly see that tunnelling through the thin AlN barrier is possible resulting in a certain electron probability density in QW2 for all states. Furthermore, we find that electrons in e1 state are basically confined in the first QW while electrons in e2 state are basically confined in the second QW. For our optically pumped devices it is essential that the absorption of light takes place in QW1 and excites electrons from the occupied e1 state to e3.

Due to the thin tunnelling barrier electron can recombine in QW2 to the unoccupied e2 state. For sample A we obtain transition energies of 0.86 eV for e1–e3 transition and 0.67 eV for e3–e2 transition. A fluctuation of the QW2 thicknesses of ±1 ML results in an e2–e3 energy shift of the order of ±100 meV. The calculated transition energies in dependence of the thickness of QW2 are shown in Fig. 2. For a fluctuation of the second QW thickness in general the e2–e3 transition is shifted, whereas the first QW thickness affects the e1–e3 transition. For the calculations we assume a doping concentration of 1×10^{20} cm^{-3} in QW1 and 5×10^{17} cm^{-3} in QW2 while the background doping in AlN is about 5×10^{18} cm^{-3}.

3.3 Structural properties The structural properties of our samples are investigated using high resolution X-ray diffraction (HRXRD). Clear SL satellites revealing the high

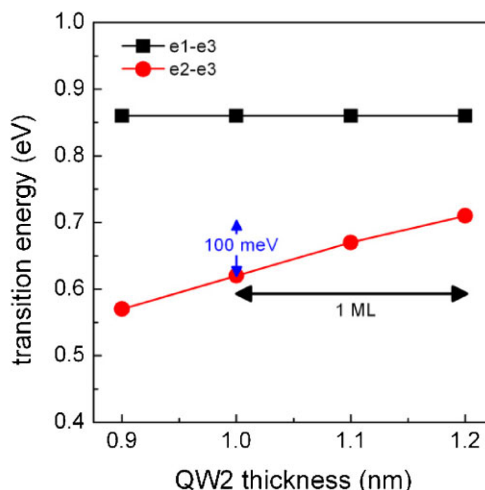

Figure 2 (online colour at: www.pss-a.com) Calculated ISBT energies for sample A for a variation of QW2 thickness.

© 2013 WILEY-VCH Verlag GmbH & Co. KGaA, Weinheim

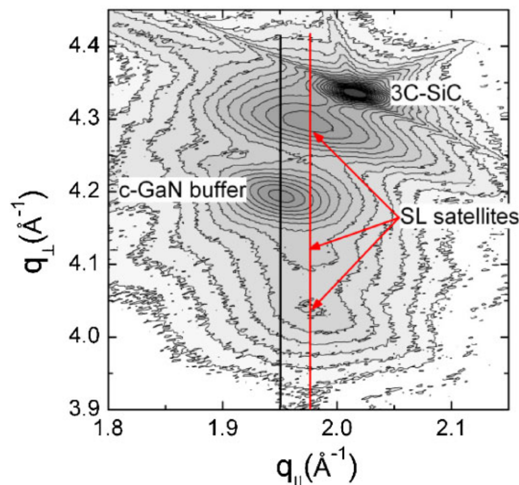

Figure 3 (online colour at: www.pss-a.com) RSM of the (113) reflection of sample B revealing clear SL satellites.

quality of the samples are detected in reciprocal space maps (RSM) of the asymmetric (113) reflection. Furthermore conclusions on the strain status of the SL can be drawn from the positions of the satellites. Figure 3 shows the RSM of the (113) reflection for sample B. The position of the satellites with respect to the position of the buffer layer indicates that the multilayer system forms an equilibrium lattice constant in between c-GaN and c-AlN. This equilibrium lattice constant results in strained GaN and AlN epilayers. This leads to compressive strained QWs and tensile strained barriers and has to be taken into account in layer thicknesses and changes in the band gap energy.

3.4 Optical properties Our MQW samples are optically investigated using cathodoluminescence (CL) and Fourier transform infrared spectroscopy (FTIR). CL probes interband transitions (IBT) while FTIR reveals ISBTs in the infrared spectral range. Figure 4 shows CL spectra of samples B and D. A clear shift of the emission maximum to higher energies is observed with narrower QWs. The broadening of the CL emission is most likely due to layer thickness fluctuations.

The infrared absorption spectrum of sample A is shown in Fig. 5. All samples show TM-polarized pronounced absorption ranging from 0.55 to 0.87 eV.

The full width at half maximum (FWHM) is about 450 meV, which is much higher than the typical broadening of 150 meV observed in single GaN/AlN QWs [7]. The shape of the absorption is asymmetric and can be fitted by two Gaussian functions. The presence of two components in the ISB absorptions can be attributed to the transitions from the ground state and from the first excited state. It is likely that the doping concentration exceeds the nominal one, so that the Fermi level is above the second energy level and the absorption from e2 to e3 can be observed.

For sample A transition energies of 0.87 eV (e1–e3) and 0.67 eV (e2–e3) are found. From the area underneath the Gaussian fit curves we conclude that the absorption e1–e3 is comparable to e2–e3 which is a hint for comparable occupation as a result of too high doping. The FWHM of individual transitions is taken from the Gaussian fit and is in the order of 200 meV for both transitions. The broadening can be explained by thickness fluctuations of the QWs which is confirmed by model calculations (see Fig. 2).

In Fig. 6, the absorption spectrum of sample B is plotted together with a fit by two Gaussian functions. The maxima of the Gaussian curves are at 0.87 and 0.63 eV, respectively. For this sample the e2–e3 absorption is found to be much weaker than the e1–e3 transition (area under curve 2 is more than a factor of 2 lower than under curve 1). This is due to a larger separation between e1 and e2 in sample B compared to sample A and therefore a larger distance to the Fermi level assuming same doping concentration for both samples. In Table 2, the experimental transition energies are summarized

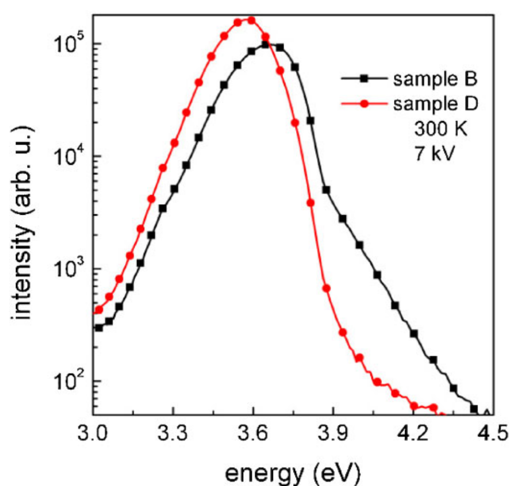

Figure 4 (online colour at: www.pss-a.com) Room temperature CL spectra of sample B (black line) and sample D (red line).

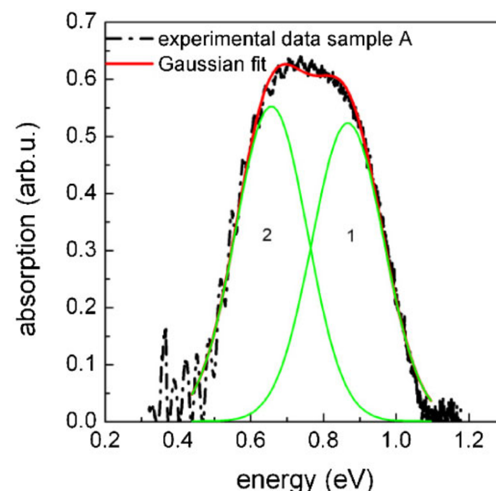

Figure 5 (online colour at: www.pss-a.com) RT absorption spectrum (black) of sample A with Gaussian fits (green) and cumulative curve (red).

© 2013 WILEY-VCH Verlag GmbH & Co. KGaA, Weinheim

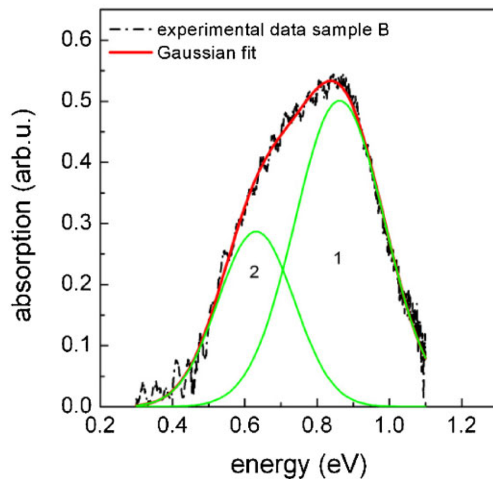

Figure 6 (online colour at: www.pss-a.com) Sample B (RT) absorption spectrum (black) with Gaussian fits (green) and cumulative curve (red).

Table 2 Calculated and measured ISBT energies.

sample	e1–e3 exp (calc.)	e2–e3 exp (calc.)
A	0.87 eV (0.86 eV)	0.67 eV (0.67 eV)
B	0.87 eV (0.87 eV)	0.63 eV (0.62 eV)
C	0.81 eV (0.82 eV)	0.63 eV (0.65 eV)
D	0.77 eV (0.77 eV)	0.55 eV (0.55 eV)

in comparison to the calculated transition energies for samples A–D. We find good agreement between measurement and calculation.

4 Conclusions Quantum confinement in asymmetric coupled GaN/AlN QWs is studied both theoretically and experimentally. ACQWs of cubic GaN/AlN were successfully grown by MBE. Intersubband absorption in the 0.55–0.87 eV range is observed at room temperature (RT). The asymmetric shape of the infrared absorptions reveals the existence of a three level system. The structures are attributed to the contributions of the e1–e3 as well as the e2–e3 transitions. This is confirmed using model calculations which reproduce transition energy and position of Fermi level reliably. The e2 state is populated due to the excessive carrier concentration, which may originate from higher background doping of AlN than estimated. Moreover the calculated transition energies for the given QW thicknesses are in good agreement with experimental data. From HRXRD results we conclude, that the MQWs form an equilibrium lattice constant in between GaN and AlN. IBTs are observed using CL. In CL spectra a clear shift to higher energies for thinner QWs is found. These results show the potential of ACQWs of cubic GaN/AlN for optically pumped ISB devices.

Acknowledgements The financial support by the German Science Foundation (DFG, project As (107/4-1)) and by European FP7 FET-OPEN project Unitrideunder grant agreement #233950 is acknowledged.

References

[1] B. Levine, J. Appl. Phys. **74**, R1 (1993).
[2] J. Faist, F. Capasso, D. L. Sivco, C. Sirtori, A. L. Hutchinson, and A. Y. Cho, Science **264**, 553 (1994).
[3] O. Gauthier Lafaye, P. Boucaud, F. H. Julien, S. Sauvage, S. Cabaret, J. M. Lourtioz, V. Thierry Mieg, and R. Planel, Appl. Phys. Lett. **71**, 3619 (1997).
[4] M. Tchernycheva, L. Nevou, L. Doyennette, F. H. Julien, F. Guillot, E. Monroy, T. Remmele, and M. Albrecht, Appl. Phys. Lett. **88**, 153113 (2006).
[5] B. Daudin, G. Feuillet, J. Hübner, Y. Samson, F. Widmann, A. Philippe, C. Bru-Chevallier, G. Guillot, E. Bustarret, G. Bentoumi, and A. Deneuville, J. Appl. Phys. **84**(4), 2295 (1998).
[6] S. V. Novikov, C. T. Foxon, and A. J. Kent, Phys. Status Solidi C **8**(5), 1439 (2011).
[7] D. J. As, Microelectron. J. **40**(2), 204 (2009).
[8] C. Mietze, M. Landmann, E. Rauls, H. Machhadani, S. Sakr, M. Tchernycheva, F. H. Julien, W. G. Schmidt, K. Lischka, and D. J. As, Phys. Rev. B **83**, 195301 (2011).
[9] E. A. DeCuir, Jr., E. Fred, M. O. Manasreh, J. Schörmann, D. J. As, and K. Lischka, Appl. Phys. Lett. **91**(4), 041911 (2007).
[10] H. Machhadani, M. Tchernycheva, S. Sakr, L. Rigutti, R. Colombelli, E. Warde, C. Mietze, D. J. As, and F. H. Julien, Phys. Rev. B **83**, 075313 (2011).
[11] C. T. Foxon, S. V. Novikov, A. E. Belyaev, L. X. Zhao, O. Makarovsky, D. J. Walker, L. Eaves, R. I. Dykeman, S. V. Danylyuk, S. A. Vitusevich, M. J. Kappers, J. S. Barnard, and C. J. Humphreys, Phys. Status Solidi C **0**(7), 2389 (2003).
[12] C. Mietze, K. Lischka, and D. J. As, Phys. Status Solidi A **209**(3), 439 (2012).
[13] F. H. Julien, A. Sa'ar, J. Wang, and J. P. Leburton, Electron. Lett. **31**, 838 (1995).
[14] A. S. Barker and M. Ilegems, Phys. Rev. B **7**, 743 (1973).
[15] J. Schörmann, S. Potthast, D. J. As, and K. Lischka, Appl. Phys. Lett. **90**, 041918 (2007).
[16] S. Birner, S. Hackenbuchner, M. Sabathil, G. Zandler, J. A. Majewski, T. Andlauer, T. Zibold, R. Morschl, A. Trellakis, and P. Vogl, Acta Phys. Polon. A **110**, 111 (2006).

© 2013 WILEY-VCH Verlag GmbH & Co. KGaA, Weinheim